Electronic Supplementary Material (ESI) for Nanoscale.

Electronic Supplementary Information

Dual wavelength lasing of

InGaN/GaN axial-heterostructure nanorod lasers

So Yeon Chun,[‡a] Gang Yeol Yoo,[‡b] Seonghyun Jeong,[a] Seung Min Park,[a] Yun Jae Eo,[c] Woong Kim,[b] Young Rag Do,*[c] and Jae Kyu Song*[a]

[a] Department of Chemistry, Kyung Hee University, Seoul 130-701, Korea

[b] Department of Materials Science and Engineering, Korea University, Seoul 136-701, Korea

[c] Department of Chemistry, Kookmin University, Seoul 136-702, Korea

* Corresponding authors. E-mail addresses: yrdo@kookmin.ac.kr; jaeksong@khu.ac.kr

Exciton-polariton model

In the exciton-polariton model,[S1-S4] the energy of the polariton is described by

$$E(\omega,k) = \hbar\omega = \hbar ck/\varepsilon(\omega)^{1/2} \quad \text{(S-1)}$$

where ω is the angular frequency, $\varepsilon(\omega)$ is the dielectric function of the medium, and k is $\sqrt{k_x^2 + k_y^2 + k_z^2}$. In this regard, the traveling wave in the exciton-polariton model is different from the classical wave in a vacuum by the factor of $1/\sqrt{\varepsilon(\omega)}$. In addition, $\varepsilon(\omega)$ in the exciton-polariton regime depends on the frequency,[S1,S2]

$$\varepsilon(\omega) = \varepsilon_\infty\left(1 + \Omega\frac{\omega_L^2 - \omega_T^2}{\omega_T^2 - \omega^2 - i\omega\gamma}\right) \quad \text{(S-2)}$$

where ε_∞ is the background dielectric constant, γ is the damping constant, Ω is the prefactor, and ω_T and ω_L are the transverse and longitudinal resonance frequencies, respectively. For the vanishing damping condition with $\hbar\omega_L$ = 3.44 eV and $\hbar(\omega_L - \omega_T)$ = 0.005 eV, $\varepsilon(\omega)$ increases steeply with approaching the resonance energy. As a result, the dispersion curve of the polariton deviates from the classical photonic model (Figure S6). Furthermore, the group velocity of the confined photons in the nanorod decreases, which appears as the enhancement of the group refractive index of the nanorod.[S3,S4] The non-classical, non-identical spectral spacing of the Fabry–Pérot modes can be explained by the energy-wavevector diagram of the exciton-polariton (Figure 4b). The mode spacing in the high energy regime is smaller, because the mode in this regime energy is closer to the exciton resonance than are the other modes.

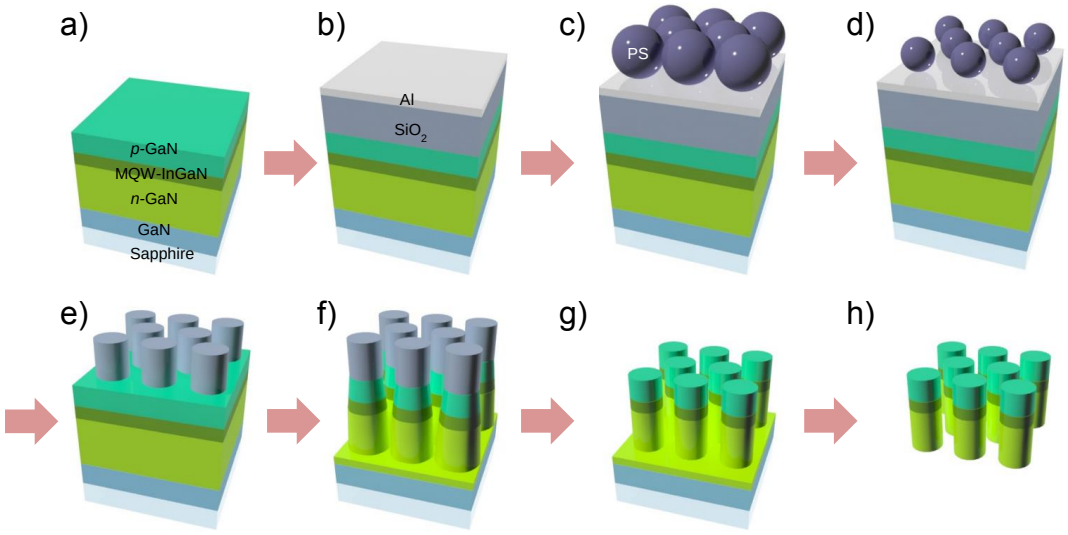

Figure S1. Schematic of fabrication procedures of InGaN/GaN nanorod array. (a) Conventional InGaN/GaN MQW-based structure on a sapphire substrate. (b) SiO_2 and Al layers deposited on GaN film. (c) Patterned monolayer polystyrene (PS) nanospheres on Al layer. (d) Ashed PS nanosphere. (e) SiO_2 nanodot layer after removal of PS following Cl_2-based reactive ion etching process. (f) SiO_2/GaN/InGaN/GaN nanorod array after etching process. (g) GaN/InGaN/GaN nanorod array after removal of SiO_2 layer. (h) Single InGaN/GaN nanorods cut from sapphire substrate.

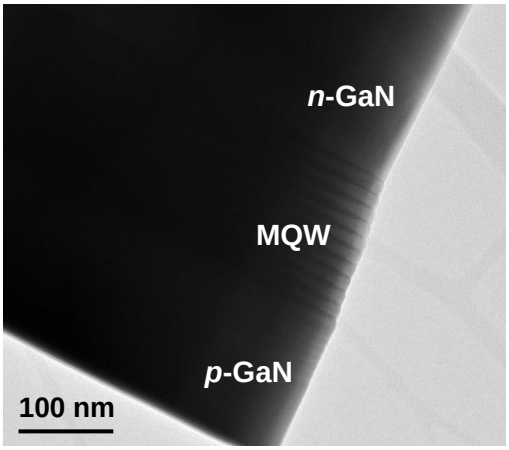

Figure S2. High-resolution TEM image of individually separated single InGaN/GaN nanorod.

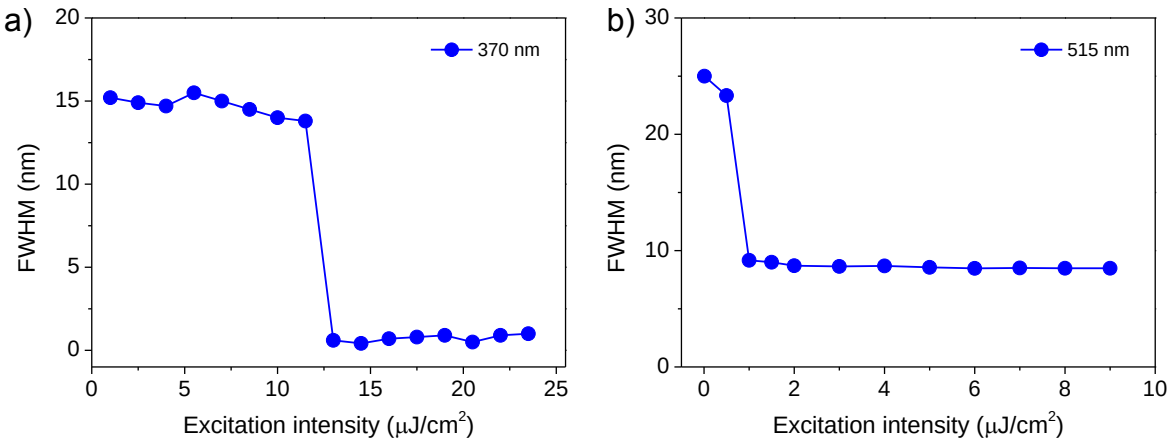

Figure S3. (a) Full-width at half-maximum (FWHM) of GaN emission as a function of excitation intensity. (b) FWHM of InGaN emission as a function of excitation intensity.

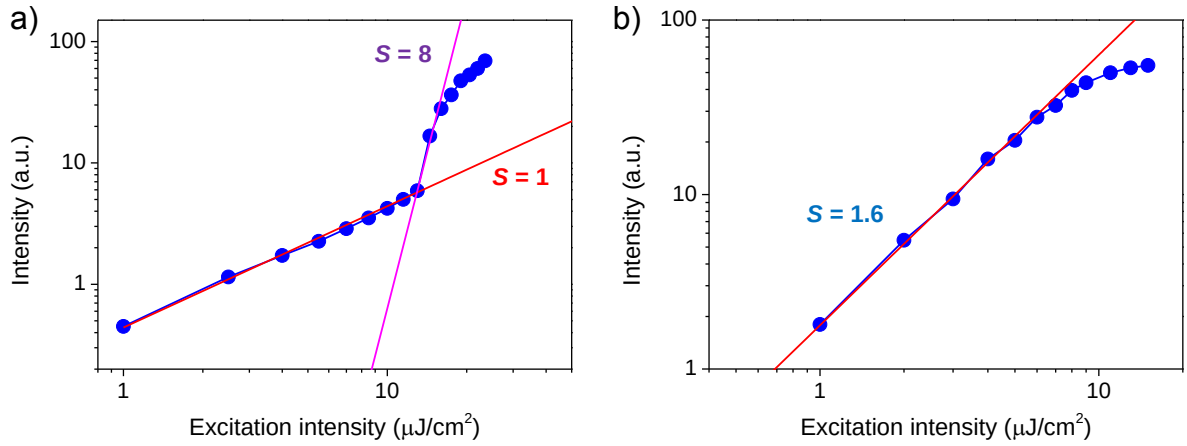

Figure S4. (a) The log-scale plot of GaN emission intensity indicates *s*-shaped curve as a function of excitation intensity. In the light-output/light-input relationship ($I_{out} = aI_{in}^{S}$), the value of S is much larger than 1 above the threshold. (b) The log-scale plot of InGaN emission intensity indicates that the value of S is larger than 1, despite saturation at the low excitation intensity.

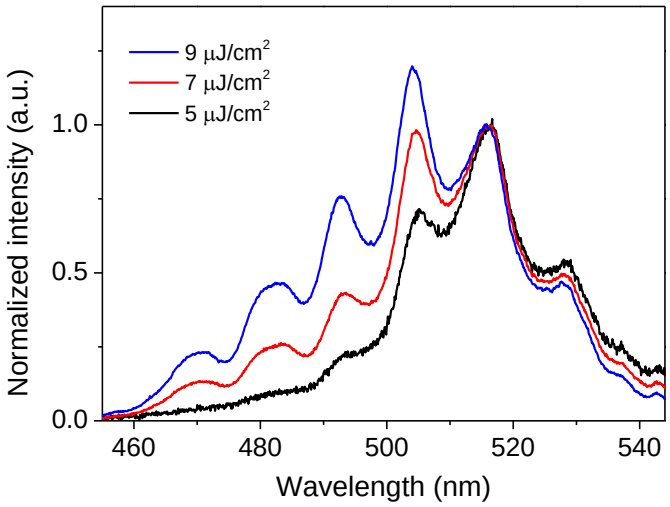

Figure S5. The emission maximum is blue-shifted with increasing excitation intensity, which leads to appearance of new modes at the high energy (short wavelength) regime at a high excitation intensity. The emission spectra are normalized for better comparison.

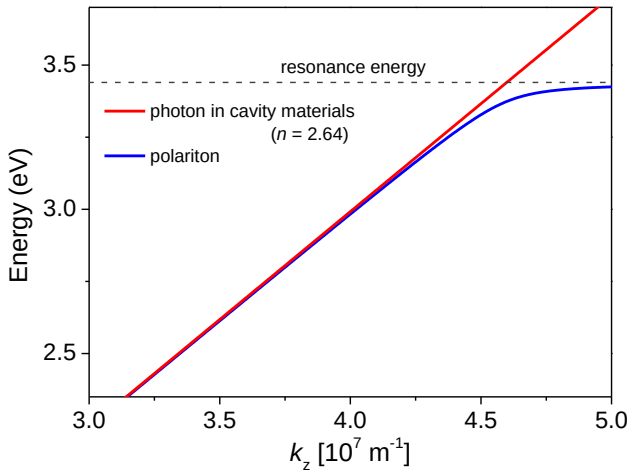

Figure S6. Comparison of the dispersion curve of traveling wave in the exciton-polariton model (blue) to that in the classical model (red).

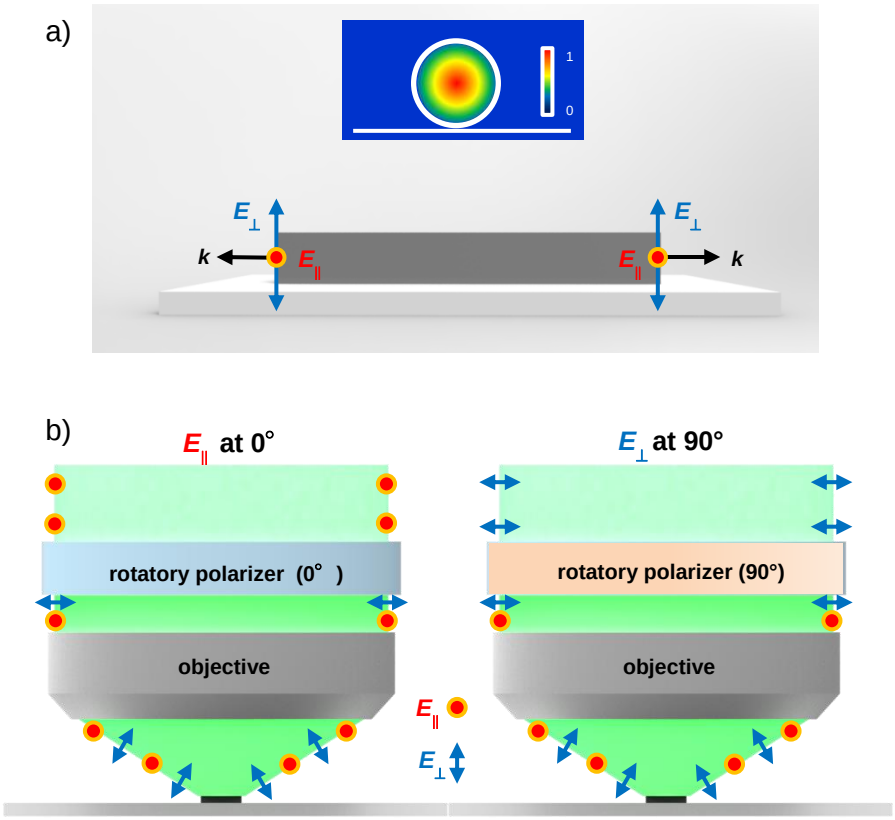

Figure S7. (a) The electric fields parallel ($\boldsymbol{E}_{\parallel}$) and perpendicular ($\boldsymbol{E}_{\perp}$) to substrate plane. The inset shows a schematic of polarization of the fundamental transverse mode. (b) $\boldsymbol{E}_{\parallel}$ is separated from $\boldsymbol{E}_{\perp}$ using a rotatory polarizer.

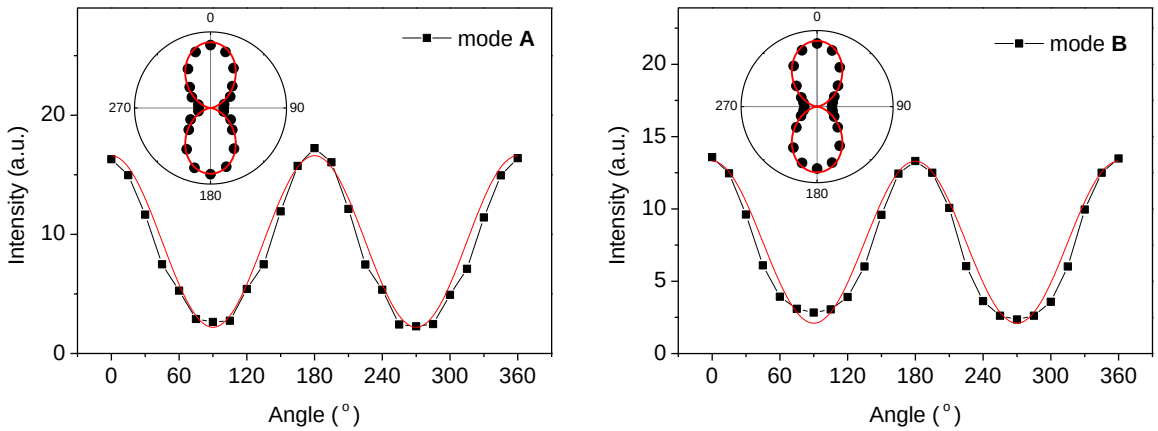

Figure S8. The degrees of polarization in modes **A** and **B** are all fitted using ρ of 0.75. The insets compare experimental data (circles) with ideal polarization ratio of $\boldsymbol{E}_{\parallel}$ mode (line).

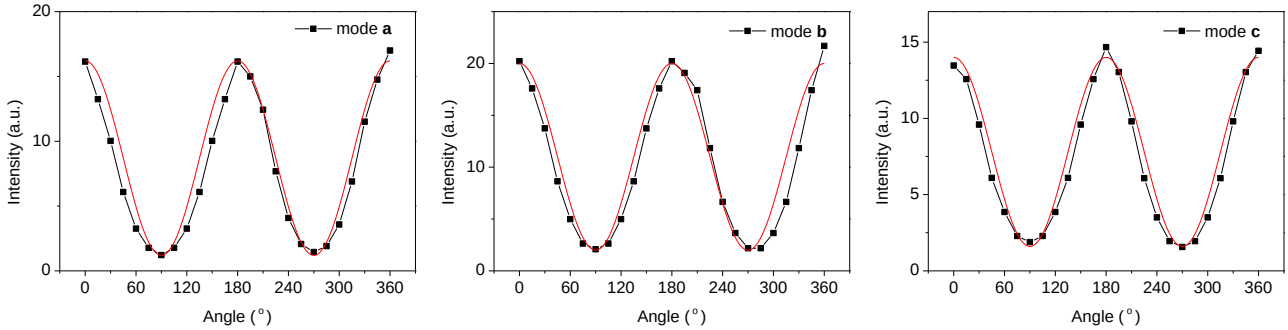

Figure S9. The degrees of polarization in modes **a**, **b**, and **c** are all fitted using ρ of 0.80.

REFERENCES

S1 S. Rühle, L. K. van Vugt, H. Li, N. A. Keizer, L. Kuipers, D. Vanmaekelbergh, *Nano Lett.*, 2008, **8**, 119-123.

S2 D. Vanmaekelbergh, L. K. van Vugt, *Nanoscale*, 2011, **3**, 2783-2800.

S3 L. K. van Vugt, B. Piccione, R. Agarwal, *Appl. Phys. Lett.*, 2010, **97**, 061115.

S4 L. K. van Vugt, B. Piccione, C. Cho, P. Nukala, R. Agarwal, *Proc. Natl. Acad. Sci. U. S. A.*, 2011, **108**, 10050-10055.